Modern Health Science; Vol. 8, No. 2; 2025
ISSN 2576-7291 E-ISSN 2576-7305
https://doi.org/10.30560/mhs.v8n2p80

Decoding the Genetic Interplay: Integrated Computational Insights into the Interplay Between Peri-Implantitis and Osteoporosis

Simin Li[1#], Deborah Kreher[2] & Gerhard Schmalz[2*]

[1] Stomatological Hospital, School of Stomatology, Southern Medical University, China

[2] Department of Conservative Dentistry and Periodontology, Brandenburg Medical School (MHB) Theodor Fontane, Brandenburg an der Havel, Germany

Correspondence: Dr. Simin Li, Stomatological Hospital, School of Stomatology, Southern Medical University, Guangzhou 510280, China. E-mail: simin.li.dentist@gmail.com

*Senior author: Prof. Dr. Gerhard Schmalz, E-mail: Gerhard.schmalz@mhb-fontane.de

Received: May 28, 2025; Accepted: June 8, 2025; Published: June 9, 2025

Abstract

Background: Peri-implantitis (PI) and osteoporosis (OP) are prevalent chronic conditions with substantial health impacts, yet the genetic and molecular links between these diseases are not fully understood. Clarifying the shared genetic similarities between PI and OP is crucial for enhancing diagnostic and therapeutic strategies.

Objective: The study aims to elucidate the shared genetic and molecular pathways between PI and OP through an integrated computational biology analysis, contributing to the development of more effective diagnostic and therapeutic approaches.

Methods: The research utilized PI-related datasets GSE33774 and GSE106090 from the GEO database and genes associated with PI and OP from DisGeNET. Differential expression analysis was conducted using the "limma" package in R. Protein-Protein Interaction (PPI) networks were constructed with Cytoscape, identifying cross-talk genes between PI and OP. The LASSO model was applied for marker gene selection and GO Biological Process and KEGG pathway analyses were conducted. Analyses of drug susceptibility and immune infiltration were also included to understand potential therapeutic implications and the role of the immune environment.

Results: The analysis identified key differentially expressed genes (DEGs) in PI and significant cross-talk genes between PI and OP. The PPI network highlighted central genes like HIF1A, TNF, TGM2, and SPP1. Marker genes (i.e., PIK3CG, SFRP4, CCR5, and PRLR) pinpointed through LASSO and logistic regression showed significant correlations with the cross-talk genes. Insights into drug susceptibility and the immune infiltration landscape in both conditions were provided. Single cell analysis further delineated the expression patterns of these marker genes in relevant cell types.

Conclusion: This study uncovers novel insights into the shared genetic landscape of peri-implantitis (PI) and osteoporosis (OP) by identifying four key marker genes—PIK3CG, SFRP4, CCR5, and PRLR—and their roles in the pathogenesis of these conditions. The integrated computational biology approach employed in this research contributes to the current body of literature by offering a deeper understanding of the genetic and molecular mechanisms underlying the interplay between PI and OP.

Keywords: peri-implantitis, osteoporosis, computational biology, Protein-Protein Interactions, Biomarker Discovery

1. Introduction

Periimplantitis (PI) and osteoporosis (OP) are increasingly recognized as interconnected conditions within the scope of bone health and disease. An increasing number of literature (1–6) has started to illuminate the potential relationships and underlying mechanisms linking these two diseases. Periimplantitis, characterized by inflammatory processes around dental implants (7,8), shares pathophysiological pathways with osteoporosis, a systemic condition marked by reduced bone density and increased fracture risk (4). The inflammatory cytokines, bone metabolism dysregulation, and immune responses are speculated to be common factors in both conditions (9–11). For instance, inflammatory mediators like TNF-α and IL-1β, elevated in PI (12), are also implicated in osteoporosis-related bone resorption processes (13). The predispositions affecting bone density and turnover might influence susceptibility to both PI and OP, hinting at a genetic connection. Additionally, the role of microbiota in

PI has been explored in relation to systemic bone loss, further linking these conditions (14,15). The impact of lifestyle factors, such as smoking and diet, on both diseases has also been investigated, suggesting a complex interplay of genetic, environmental, and lifestyle factors in their pathogenesis (16,17).

Although there appears to be an increasing body of clinical evidence, it remains unclear, how PI and OP are genetically and molecularly connected. Most studies have only looked at correlations between these conditions. Focused on specific aspects of their underlying mechanisms giving us a fragmented understanding of the overall genetic landscape. This research aims to bridge that gap by using computational biology analysis to uncover the shared pathways and molecular mechanisms between periimplantitis and osteoporosis. What sets this study apart is its faceted approach, combining gene expression data, protein-protein interaction networks, and advanced statistical models. By taking this approach, the aim of the current research is to gain a holistic understanding of how these diseases interact with each other, potentially revealing new biomarkers and targets for therapy. This methodology aligns with the growing trend of using tools in biomedical research and responds to calls for more integrated approaches in tackling complex diseases. Moreover, the use of bioinformatics tools and algorithms in this study represents a significant advancement, in unraveling the intricate genetic networks underlying these conditions.

Recent advancements in bioinformatics have opened new avenues for understanding the complex relationships between seemingly distinct diseases. By leveraging high-throughput data and computational tools, researchers can uncover shared molecular pathways, genetic risk factors, and potential therapeutic targets. This approach has been successfully applied to various disease pairs, revealing unexpected connections and informing novel treatment strategies. For instance, a recent study by Li et al. (2021) employed bioinformatics techniques to investigate the similarity and potential relationship between peri-implantitis and rheumatoid arthritis at the transcriptomic level (18). The study identified common differentially expressed genes and signaling pathways, suggesting a shared inflammatory etiology and potential therapeutic targets. Similarly, bioinformatics approaches have shed light on the molecular links between periodontitis and systemic diseases such as psoriasis (19), venous thromboembolism (20), Parkinson's disease (21), and type 2 diabetes (22). These studies demonstrate the power of bioinformatics in unraveling the complex interplay between oral and systemic health, paving the way for personalized medicine and targeted interventions. In the context of peri-implantitis and osteoporosis, applying bioinformatics techniques could provide invaluable insights into their shared genetic underpinnings, inflammatory pathways, and potential therapeutic strategies, ultimately improving patient care and outcomes.

The primary objective of this study is to examine the relationship between PI and OP at a genetic and molecular level. By employing computational biology techniques, it was aimed to analyze gene expression data from the GEO database and gene associations from DisGeNET. Through this research genetic pathways and biomarkers should be identified, which are shared between these two conditions. The analysis involved constructing Protein Protein Interaction (PPI) networks using Cytoscape and utilizing LASSO logistic regression models. These methodologies will play a role in uncovering potential targets for therapeutic intervention as well as enhancing the understanding of how PI and OP develop together. This study represents a step forward, in this field of research. Thereby, it was hypothesized that by applying advanced bioinformatics techniques to analyze gene expression data, we will uncover shared genetic pathways, potential biomarkers, and therapeutic targets that underlie the complex interplay between peri-implantitis and osteoporosis. Furthermore, we postulate that the identification of these common molecular mechanisms will provide a foundation for the development of novel diagnostic tools and targeted treatment strategies, ultimately leading to improved patient care and outcomes in the management of these debilitating conditions.

2. Material and Methods

2.1 Data Downloading

Peri-implantitis (PI)-related datasets (GSE33774 and GSE106090) were downloaded from the GEO database (http://www.ncbi.nlm.nih.gov/). For both datasets, PI-related and control samples were selected for inclusion in the subsequent analysis. Sample information statistics for GSE33774 and GSE106090 are shown in Table 1. Additionally, osteoporosis (OP)-related gene sets and PI-related genes were obtained from the DisGeNET database (http://www.disgenet.org). In total, 1,098 OP-related gene sets and 63 PI-related gene sets were acquired for further analysis.

Table 1. The statistical information of GSE33774 and GSE106090 datasets

	GSE33774	GSE106090
Experiment type	Array	
Platforms	GPL6244	GPL21827
Case	7	6
Control	8	6

2.2 Data Processing

For the PI datasets (GSE33774, GSE106090), the Probe IDs were first converted to Gene Symbols. The human gene annotation dataset was obtained from GENCODE (https://www.gencodegenes.org/human/), and the mapping relationship between Probe ID and Gene Symbol was obtained based on the Probe ID information and the human gene annotation dataset provided by the platform. The IDs in GSE33774 and GSE106090 were replaced with Gene Symbols, and Gene Symbols with possible duplicates were de-weighted using gene expression averages. Any Gene Symbol was removed when the number of samples with an expression value of 0 exceeded 50% of the total number of samples. Finally, log2 scaling was performed on GSE33774, which had a large difference in sample expression values.

For the PI datasets (GSE33774 and GSE106090), the first step involved converting the Probe IDs to Gene Symbols. To accomplish this, the human gene annotation dataset was obtained from GENCODE (https://www.gencodegenes.org/human/). The mapping relationship between Probe IDs and Gene Symbols was then established based on the Probe ID information and the human gene annotation dataset provided by the platform. Subsequently, the IDs in GSE33774 and GSE106090 were replaced with their corresponding Gene Symbols. In cases where Gene Symbols had potential duplicates, gene expression averages were used to de-weight them. Furthermore, any Gene Symbol was removed if the number of samples with an expression value of 0 exceeded 50% of the total number of samples. Lastly, log2 scaling was performed on GSE33774 to address the large differences in sample expression values.

2.3 PI Dataset Variance Analysis

For the PI datasets (GSE33774 and GSE106090), the "limma" package in R (version 4.1.3) (23) was employed to analyze the differences between the Case and Control samples. By comparing the gene expression values across different groups, it is possible to identify genes with significant differences, which are labeled as differentially expressed genes (DEGs). The determination of significant differences in gene expression relies on two reference factors: the P-value and the log fold change (FC) value. In this study, genes with a P-value < 0.05 and an absolute log FC value > 1 were considered as DEGs.

2.4 PI and OP Cross-Talk Gene

GSE33774 and GSE106090 co-differentially expressed genes were obtained, which are considered to be genes with consistent and stably varying expression trends in PI. The co-differentially expressed genes were merged with the PI-related genes downloaded from the DisGeNET database, resulting in a set of PI potentially related genes. Finally, the common genes between the PI potentially relevant gene set and the OP relevant gene set were extracted, which are considered as the cross-talk genes of PI and OP. The expression of these cross-talk genes in PI was extracted and visualized in a heatmap using the pheatmap package of the R language (24). Subsequently, the clusterProfiler package in R was employed to analyze the GO biological processes and KEGG pathways, to obtain the biological functions affected by the cross-talk genes.

2.5 Protein Interaction (PPI) Network Analysis of Cross-talk Gene

Protein-protein interaction (PPI) pairs between cross-talk genes and other genes were obtained from the HPRD database (http://www.hprd.org/) and the BIOGRID database (http://thebiogrid.org/). The PPI data obtained from these two databases were combined, resulting in the final cross-talk gene-related PPIs. The cross-talk gene-related PPI network was constructed using Cytoscape (version 3.9), and NetworkAnalyzer (https://med.bioinf.mpi-inf.mpg.de/netanalyzer/help/2.7/index.html#complex) was employed to analyze the topological properties of the PPI network.

2.6 Screening of Marker Genes for PI and OP

To further screen the bridge genes that play more important roles in PI and OP, the cross-talk genes were subjected to additional filtering. Initially, the two PI datasets (GSE33774 and GSE106090) were merged based on their common genes to obtain the merged gene expression profiles. Subsequently, the expression values of cross-talk

genes were extracted from the merged profiles, and the features of these genes were filtered using the LASSO (Least absolute shrinkage and selection operator) model. The LASSO model can be constructed to obtain a more refined model by incorporating a penalty function, which changes the regression coefficients of unimportant features to 0, thereby facilitating the selection of hub genes. The analysis results provide two optional parameters: lambda.min, which is the value of lambda that gives the minimum cross-validation mean (cvm), and lambda.1se, which is the largest value of lambda such that the error is within 1 standard error of the minimum. In this study, the result of lambda.min was chosen to filter the cross-talk genes. Finally, univariate logistic regression was employed to further screen the results of the LASSO analysis, and genes with a P-value < 0.05 in the univariate logistic regression results were defined as marker genes for PI and OP.

2.7 Building a Multivariate Logistic Prediction Model

The expression values of marker genes were extracted from the combined PI expression profile, and the samples were randomly divided into training and test sets at a ratio of 6:4, with 60% of the samples used for training and the remaining 40% for testing. A multivariate logistic regression model was constructed based on the rms package (25) to analyze the marker gene expression matrix of the training set. The model-derived Linear Predictor Score of the training set was then subjected to an inverse logit transformation using the rms package to obtain the Risk Score for each sample. Finally, a nomogram was constructed using the rms package to illustrate the relationship between the marker genes and the Risk Score.

The R language nomogramFormula package (26) was used to obtain all the sample Total Points from the nomogram table. These Total Points were then incorporated into the Decision Curve Analysis (DCA) as the model measure. Additionally, the top two marker genes that had a greater impact on the Risk Score were identified from the nomogram table. The expression values of these top two marker genes were used as the gene measure and incorporated into the DCA to provide a better reference for clinical decision-making.

To validate the predictive performance of the logistic prediction model, the calibration curve was first calculated using the calibrate method in the rms package. Subsequently, all the samples of marker genes in the PI expression matrix, including both the training and test sets, were incorporated into the model for prediction. ROC analysis was then performed based on the sample type and the sample Risk Score to evaluate the model's predictive accuracy.

2.8 Marker Gene Correlation and Expression Level Analysis

To investigate the relationship between marker genes and cross-talk genes, the expression values of marker genes and cross-talk genes were first extracted from the PI disease samples. The relationship between the expression levels of marker genes and cross-talk genes was then analyzed using Pearson correlation coefficients. Simultaneously, the Risk Scores of the PI disease samples were extracted, and Pearson correlation coefficients were used to predict the relationship between marker genes and Risk Scores.

Box-and-line plots were employed to illustrate the expression levels of marker genes in both Case and Control samples of PI. Additionally, the Wilcoxon test was used to analyze the significant relationship of marker genes between the two groups of samples. Finally, ROC analysis was performed on marker gene expression values based on Case-Control sample types to evaluate their diagnostic potential.

2.9 Constructing Marker Gene-Related PPI-Pathway Network

PPI relationship pairs of marker genes were extracted from the cross-talk gene-related PPI network and labeled as marker gene-Target 1 relationship pairs. All the pathways and their associated genes were then obtained from the KEGG database (https://www.kegg.jp/). The pathways related to the marker genes were extracted, resulting in the selected marker gene-pathway relationship pairs. Subsequently, all the genes under the pathways in the marker gene-pathway relationship pairs were extracted to obtain the pathway-Target2 relationship pairs. The marker gene-pathway relationship pairs and the pathway-Target2 relationship pairs were constructed using pathways as the connecting medium. Genes in Target1 were then screened from the Target2 gene set to form the Target1-marker gene-pathway-Target1 closed-loop structure. Finally, Cytoscape was employed to construct the Target1-marker gene-pathway-Target1 closed-loop structure network.

2.10 Drug Susceptibility Analysis of Marker Gene

To predict sensitive drugs for the treatment of peri-implantitis and osteoporosis, drug sensitivity data and RNA-seq data for compounds were downloaded from the Cell Miner database (https://discover.nci.nih.gov/cellminer/home.do). Drugs that had undergone clinical trials (Clinical trial) and received FDA approval (FDA approved) were selected for further analysis. The expression values of marker genes were extracted, and Pearson correlation coefficients were calculated to determine the correlation between the

expression of each marker gene and different drugs. This analysis was then used to evaluate the drug sensitivity of the marker genes.

2.11 Immune Infiltration Analysis

To analyze the potential immune cells associated with PI and OP, CIBERSORT analysis was employed. CIBERSORTx (https://cibersortx.stanford.edu/) analyzes gene expression profiles based on a known reference dataset, the official gene expression signature set for 22 immune cell subtypes: LM22. Since no expression profiles were available for OP, the expression profile dataset of PI was used for immune infiltration analysis. Potentially relevant immune cells for OP were predicted by immune cells highly expressed with PI. CIBERSORT analysis was performed based on the PI expression matrix and LM22 dataset to obtain a matrix of cell abundance scores for 22 immune cell subtypes in each sample, as well as the significance and correlation between each sample and the corresponding sample of the expression profile. Samples with P-value < 0.05 were chosen as the samples that were significantly correlated with the immune cell signature set and PI. Finally, the Wilcoxon test was used to analyze the variability of immune cells across sample types.

The significantly different immune cell abundance scoring matrices from the Wilcoxon test were extracted, and Pearson correlation coefficients were used to predict the correlation between significantly different immune cells and other immune cells. Additionally, samples from the marker gene expression matrix that were common to the immune cell scoring matrix were extracted, and Pearson correlation coefficients were used to predict the relationship between significantly different immune cells and the marker genes.

2.12 Expression Analysis of Marker Genes in Single Cells of Bone and PBMC and Pathway Mapping

To further analyze the expression of marker genes in cell lines, the results of single-cell analysis of marker genes in bone and PBMC were downloaded from the HPA database (https://www.proteinatlas.org/). Additionally, the functional relationships of marker genes in important pathways were analyzed. Important pathways and their associated genes were downloaded from the KEGG database, and the marker genes were mapped to the KEGG pathways using the R language pathview package (27).

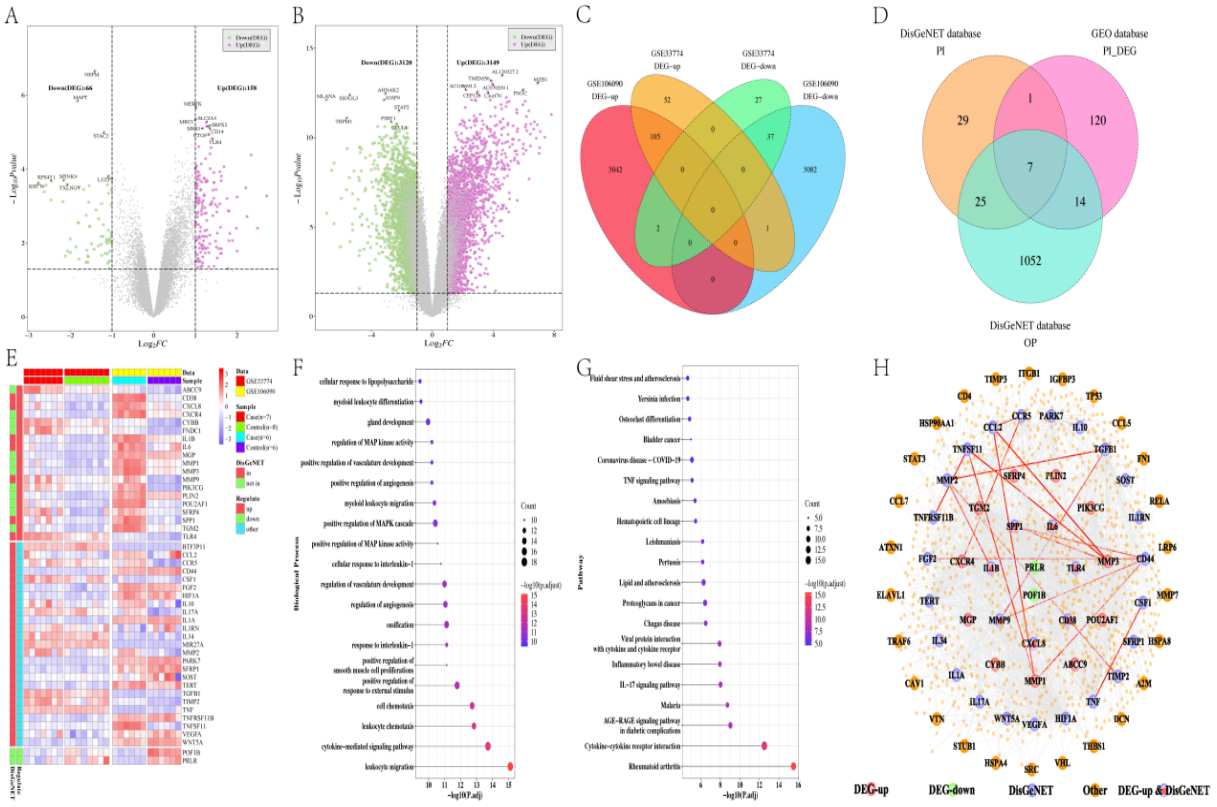

Figure 1. The identification of differentially expressed genes and crosstalk genes

(A) GSE33774 differentially expressed analysis volcano map; (B) GSE106090 differentially expressed gene volcano map; (C) Statistics of differentially expressed genes of PI; (D) Statistics of the number of cross-talk genes; (E) Cross-talk gene heatmap; (F-G) GO biological process (F) and KEGG pathway enrichment analysis (G) of

cross-talk genes; (H) Cross-talk gene related PPI network. The other nodes with lower Degree in the network were hided; only the nodes with higher Degree and the 43 Cross-talk genes were remained and displayed; andred edge markers were used for the nodes with interactions between Cross-talk genes.

3. Results

3.1 PI and OP Cross-Talk Gene Screening

By analyzing the PI dataset, genes with P-value < 0.05 and |logFC| > 1 were selected as DEGs, where logFC > 1 represents up-regulated genes and logFC < -1 represents down-regulated genes. The number of differentially expressed genes was obtained (see Table 2). Volcano plots were used to visualize the distribution of DEGs in the two datasets (GSE33774 (Fig 1A) and GSE106090 (Fig 1B)), with the top 8 up-regulated and down-regulated genes labeled according to their P-values.

Table 2. Relevant statistics for differential expression analysis of PIs

	GSE33774	**GSE106090**
Limma analysis results		
P value	P < 0.05	
|Log2(FC)|	|Log2(FC)| > 1	
Up number	158	3149
Down number	66	3210
Total	224	6359

Differential analysis of PI yielded 224 DEGs from GSE33774 and 6,359 DEGs from GSE106090. A total of 142 genes with consistent expression trends were finally obtained, including 105 up-regulated genes and 37 down-regulated genes (Fig 1C). The DisGeNET database provided 63 PI-related genes, and a total of 196 genes were obtained by taking the concatenated set of 142 PI differentially expressed genes and 63 known PI genes, which were considered potential disease genes for PI. The DisGeNET database also provided 1,098 OP-related genes. The intersection of the 196 PI-related genes and 1,098 OP-related genes was taken, and the intersecting genes were considered potential cross-talk genes for PI and OP. Finally, 46 cross-talk genes were obtained, among which 7 genes (CD38, CXCL8, IL1B, IL6, MMP9, SPP1, TLR4) were present in all three datasets simultaneously (Fig 1D). The expression of the 46 cross-talk genes in GSE33774 and GSE106090 was extracted (Fig 1E).

The clusterProfiler package in R was used to perform GO Biological Process (Fig 1F) and KEGG pathway (Fig 1G) analyses on these 46 cross-talk genes, with functions having a P.adjust < 0.05 considered significant. The top 20 significant functions were displayed. According to the enrichment results, cross-talk genes are mainly involved in leukocyte migration, cytokine-mediated signaling pathways, response to interleukin-1, ossification, and positive regulation of MAP kinase activity, among other biological processes (Fig 1F). Additionally, these genes regulate the IL-17 signaling pathway, TNF signaling pathway, and osteoclast differentiation (Fig 1G).

By combining data from the HPRD and BIOGRID databases, protein interaction relationship pairs of cross-talk genes were obtained, and a PPI network for these relationship pairs was constructed using Cytoscape software (Fig 1H). This process yielded 1,327 cross-talk gene-related PPIs, involving a total of 1,073 genes, including 43 cross-talk genes. The topological properties of the PPI network were analyzed and arranged in descending order based on degree. The top 25 genes were selected for display (Table 3), revealing that HIF1A, TNF, TGM2, and SPP1 were among the most regulated genes in the network.

3.2 Obtainment and Multivariate Logistic Analysis of Marker Genes

LASSO was used to screen 46 cross-talk genes (Fig 2A-B), resulting in the identification of eight cross-talk genes (PIK3CG, PLIN2, SFRP4, TLR4, CCR5, IL1RN, WNT5A, PRLR) based on the lambda.min parameter. Univariate logistic regression was then performed on these eight cross-talk genes, and genes with a P-value < 0.05 in the univariate logistic regression results were selected as marker genes (Fig 2C). After screening, four marker genes (PIK3CG, SFRP4, CCR5, PRLR) were finally obtained. Among them, the aberrant expression of PIK3CG, SFRP4, and CCR5 (OR > 1) may promote disease progression, while the aberrant expression of PRLR may slow down the disease progression.

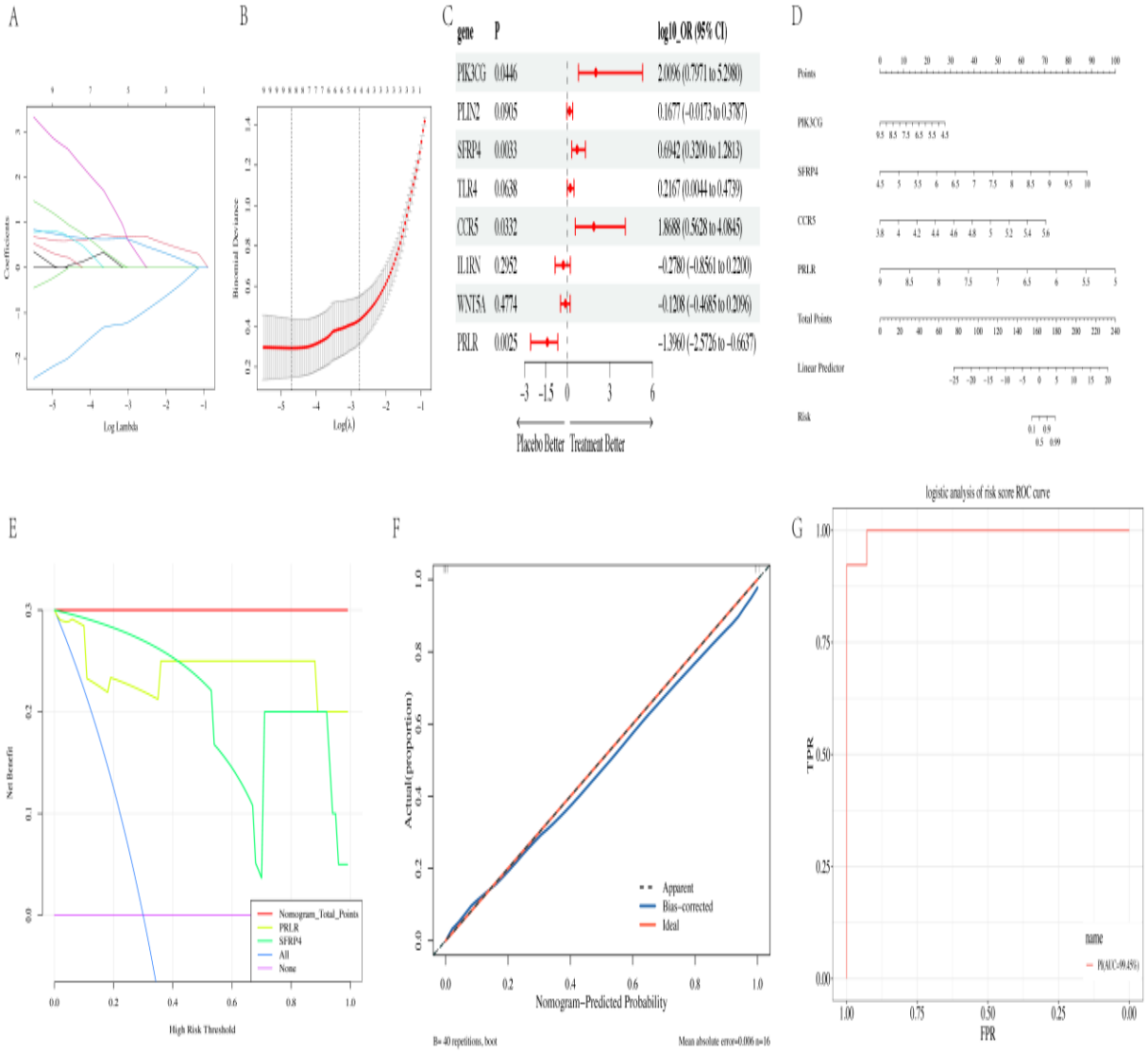

Figure 2. Marker gene screening

(A) Results of LASSO analysis, each line in the figure represents a gene, when the gene tends to 0 the larger value of the horizontal coordinate (Log Lambda) indicates the more critical gene. (B) Results of model cross-validation. There are two dotted lines in the figure, one is the λ value lambda.min when the mean square error is the smallest, and the other is the λ value lambda.1se when the distance from the mean square error is the smallest by one standard error, these two values can be chosen either way, and the numbers corresponding to the dotted lines are the results of the number of screened genes, and here we choose the lambda.min as the screening condition of the marker gene. (C) Logistic regression results. Since OR greater than 1 is a risk factor and vice versa is a protective factor. We scaled log10 for both OR and 95% confidence interval in the figure, and log10(1) = 0, so the dotted line in the middle is on 0. (D) Total Points are obtained by calculating the Points values of the sample elements, and the corresponding risk value of the sample is under the Total Points. For example, if the PIK3CG expression value of four genes in a sample is 6, then the corresponding Points score is about 20, and the other three are similarly calculated, and the sum of the four Points scores is the Total Points. (E) The horizontal line None indicates the case when all the people don't receive the treatment, and the benefit is zero regardless of the High Risk Threshold. The dotted line All represents the change in net benefit with the change in High Risk Threshold when everyone receives treatment. These two lines represent 2 extreme cases. For a given probability threshold, the larger the net benefit, the better, so the curve is generally as far away from the two particular lines as possible. (F) Calibration curve of the model. (G) ROC Analysis.

Table 3. Topological property analysis of top 20 Cross-talk gene. AverageShortestPathLength (ASPL), Betweenness centrality (BC), Closeness centrality (CC), Topological coefficients (TC).

Symbol	Degree	ASPL	BC	CC	TC
HIF1A	156	2.802337	0.283285	0.356845	0.019477
TNF	103	2.956183	0.191842	0.338274	0.01607
TGM2	100	2.964946	0.177729	0.337274	0.022308
SPP1	90	3.081792	0.149647	0.324487	0.013808
PARK7	76	3.198637	0.11916	0.312633	0.035088
TGFB1	72	3.222006	0.115771	0.310366	0.020556
TERT	70	3.226874	0.107644	0.309897	0.04
CD44	68	2.839338	0.16307	0.352195	0.018953
CCR5	44	3.51704	0.067005	0.28433	0.033117
TLR4	42	3.364167	0.072127	0.29725	0.059524
CXCR4	40	3.463486	0.062313	0.288726	0.038182
MMP2	38	3.137293	0.057518	0.318746	0.036662
TNFSF11	38	3.32814	0.061883	0.300468	0.036636
FGF2	35	3.24148	0.051027	0.308501	0.032911
PIK3CG	33	3.989289	0.067943	0.250671	0.030303
MMP9	32	3.293087	0.046237	0.303666	0.037931
VEGFA	31	3.370983	0.043082	0.296649	0.057604
MMP3	26	3.425511	0.040621	0.291927	0.045897
CCL2	22	3.395326	0.037469	0.294523	0.054324
PRLR	21	3.650438	0.02489	0.27394	0.089947
IL1B	21	3.424537	0.028732	0.29201	0.060952
MMP1	18	3.529698	0.020026	0.28331	0.066138
SFRP4	18	1	1	1	0
POU2AF1	17	4.375852	0.027723	0.228527	0.058824
POF1B	14	4.199611	0.020291	0.238117	0.119048

The expression values of the four marker genes were extracted, and the samples in the expression matrix were randomly divided into a training set (60% of the samples) and a test set (40% of the samples). A multivariate logistic regression model was constructed to analyze the marker gene expression matrix of the training set. Using the plogis method from the R language stats package, the inverse logit of the model's Linear Predictor Score was calculated to obtain the Risk Score. A nomogram table was used to show the relationship between the marker genes and the Risk Score (Fig 2D). The results revealed that SFRP4 and PRLR have a large impact on Total Points (Fig 2D). The training set sample Total Points from the nomogram table, as well as the top two marker genes (SFRP4 and PRLR) that had a greater impact on Risk Score, were obtained for inclusion in the DCA analysis. Clinical decision curves showed that as the High-Risk Threshold increased, the Net Benefit for Total Points was superior to SFRP4 and PRLR, with higher overall net benefit observed over a wide range of thresholds (Fig 2E). To verify the multivariate logistic model's prediction effect, the calibration curve of the model was first calculated. The calibration curve was found to be close to the Actual Proportion in the model's Predicted Probability, indicating that the calibration curve does not deviate significantly from the corresponding reference line (Fig 2F). The model was then used to predict all the samples, and ROC analysis was performed on the prediction result Risk Score to assess the model's prediction effect (Fig 2G). As a result, the AUC value of the model was obtained to be 0.99, indicating that the logistic model established by the four marker genes has a good prediction effect on PI and that there is a significant difference between the expression values of the Case and Control samples for the four marker genes.

3.3 Marker Gene Correlation Analysis

Pearson's correlation coefficient was used to calculate the correlations between the 4 marker genes and the 46 cross-talk genes (including the four marker genes) (Fig 3A). Relationship pairs with $|cor| > 0.7$ were extracted, and the results showed that CCR5 was significantly positively correlated with POF1B (cor = 0.7622); PIK3CG was significantly positively correlated with POU2AF1, CXCL8, etc. (cor > 0.7) and significantly negatively correlated with IL34 and IL1RN (cor < -0.85); SFRP4 was highly positively correlated with MMP2 (cor = 0.7913) and significantly negatively correlated with POF1B (cor = -0.7107) (Table 4). Correlation analysis between marker genes and sample risk scores revealed that PIK3CG, SFRP4, and CCR5 were positively correlated with sample

risk scores, while PRLR was negatively correlated with sample risk scores (Fig 3B-E). Gene expression analysis showed that the expression levels of PIK3CG, SFRP4, and CCR5 in the Case samples were significantly higher than those in the Control samples, while the expression level of PRLR in the Case samples was significantly lower than that in the Control samples (Fig 3F-G). The AUC values of the 4 marker genes were greater than 80%, indicating that these four genes had a relatively good prediction effect (Fig 3H).

Table 4. Significantly correlation between marker genes and cross talk genes

Marker gene	**Corss_talk gene**	r value	**Pvalue**
PIK3CG	POU2AF1	0.8947	3.64E-05
PIK3CG	CXCL8	0.8287	0.000463
PIK3CG	CD38	0.8130	0.000728
PIK3CG	CXCR4	0.7838	0.001522
PIK3CG	MMP1	0.7455	0.003441
PIK3CG	IL1B	0.7209	0.005426
PIK3CG	TNFRSF11B	0.7173	0.005784
PIK3CG	TGM2	0.7135	0.006168
PIK3CG	PARK7	0.7041	0.007219
PIK3CG	SPP1	0.7040	0.007237
PIK3CG	MIR27A	-0.7022	0.00745
PIK3CG	IL1RN	-0.8077	0.000839
PIK3CG	IL34	-0.8126	0.000736
SFRP4	MMP2	0.7913	0.001272
SFRP4	POF1B	-0.7107	0.006466
CCR5	POF1B	0.7622	0.002454

118 Marker gene-Target1 relationship pairs were obtained from the PPI network. Based on the KEGG database, 6970 Marker gene-Pathway-Target2 relationship pairs were extracted. Screening genes in Target1 from the Target2 gene set yielded a total of 452 Target1-Marker gene-Pathway-Target1 closed-loop structures. A marker gene-related network was constructed using Cytoscape (Fig 3I). The network contains 100 nodes and 509 edges, which include 4 Marker genes, 2 cross-talk genes, 69 Target genes, and 25 Pathways. From the network, it can be observed that PIK3CG is involved in the PI3K-Akt signaling pathway, Apelin signaling pathway, Oxytocin signaling pathway, Chemokine signaling pathway, and other pathways. CCR5 is involved in the Chemokine signaling pathway and Cytokine-cytokine receptor interaction pathway. PRLR is involved in the Cytokine-cytokine receptor interaction pathway, JAK-STAT signaling pathway, Prolactin signaling pathway, PI3K-Akt signaling pathway, and others. SFRP4 is involved in the Wnt signaling pathway.

3.4 Drug Susceptibility Analysis of Marker Gene

The prediction of drug sensitivity allows the identification of potential responding drugs for diseases. Drug sensitivity data in different cell lines and RNA-seq data of genes in different cells were obtained from the CellMiner database. The correlation between the 4 marker genes and different drugs was calculated. Pairs with a p-value < 0.05 and a correlation greater than or equal to 0.3 were selected as significant relationships. The top 3 drugs that were significantly correlated with each marker gene were extracted and presented (Fig 4A-L). The drugs that were analyzed to have a high positive association with CCR5 were AM-5992, Megestrol acetate, and PF-2771 (Fig 4A-C). Drugs highly positively correlated with PIK3CG were auranofin, Carmustine, and Ifosfamide (Fig 4D-F). Drugs highly positively correlated with PRLR were Cilengitide, Olaparib, and PKI-587 (Fig 4G-I). Drugs highly positively correlated with SFRP4 were Caffeic acid, CEP-9722, and JNJ-38877605 (Fig 4J-L).

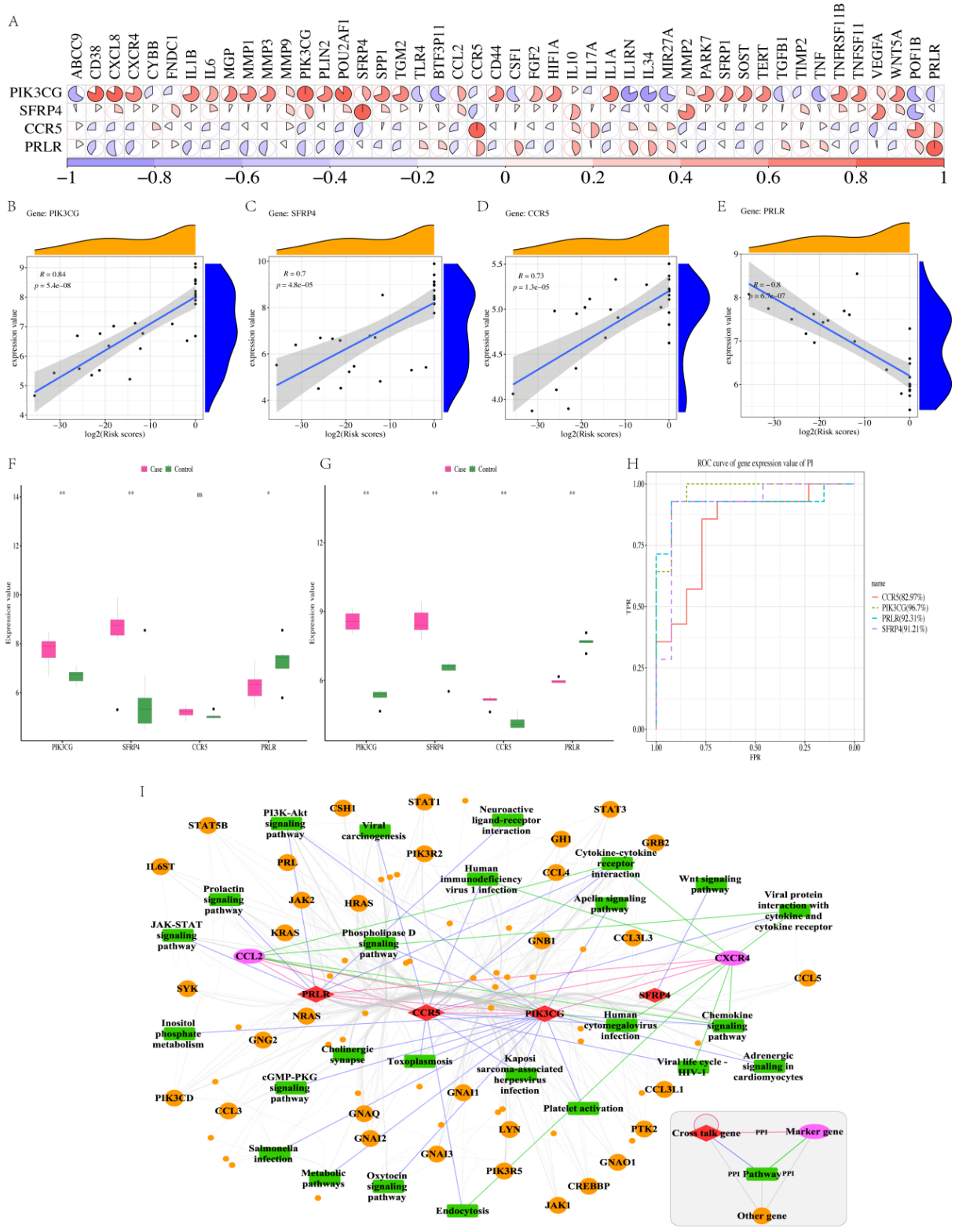

Figure 3. The relationship between marker genes and crosstalk genes

(A) Marker gene and cross-talk gene correlation analysis; (B-E) The correlation between sample risk scores and four marker genes; (F-G) Expression level of marker gene in PI two data sets. the smaller the Pvalue value of Wilcoxon test result, the more significant the sample difference result, the more "*" on the graph, the P value and the "*" sign The correspondence is ns: p > 0.05, *: p <= 0.05, **: p <= 0.01, ***: p <= 0.001, ****: p <= 0.0001. (H) ROC analysis of marker gene. (I) Marker gene-related pathway-PPI network.

The samples were categorized into high-risk and low-risk groups according to the median value of gene expression in the RNA-seq data for each marker gene. The scores of high-risk and low-risk groups in the drug sensitivity data were obtained. Differences between samples from different risk groups in the drug sensitivity data were analyzed using t-test, and the box-and-line plot shows the results of the gene and associated drug analysis in Fig4A-L (Fig 4M-Y). For CCR5 and PIK3CG, the high-risk groups exhibited high sensitization activity for each of the three drugs of interest (Fig 4M-R). Olaparib and PKI-587 had low sensitization activity in the PRLR high-risk group (Fig 4U-V), while Cilengitide had low activity in both high and low-risk groups (Fig 4S). The three drugs highly positively correlated with SFRP4 did not differ in activity between the high and low-risk groups (Fig 4W-Y). Each drug and its multiple significantly related marker genes were extracted for network mapping (Fig 4Z). The results showed that BLU-667 was significantly positively correlated with PRLR, and negatively correlated with PIK3CG. Camptothecin was significantly positively correlated with PIK3CG, SFRP4, and CCR5.

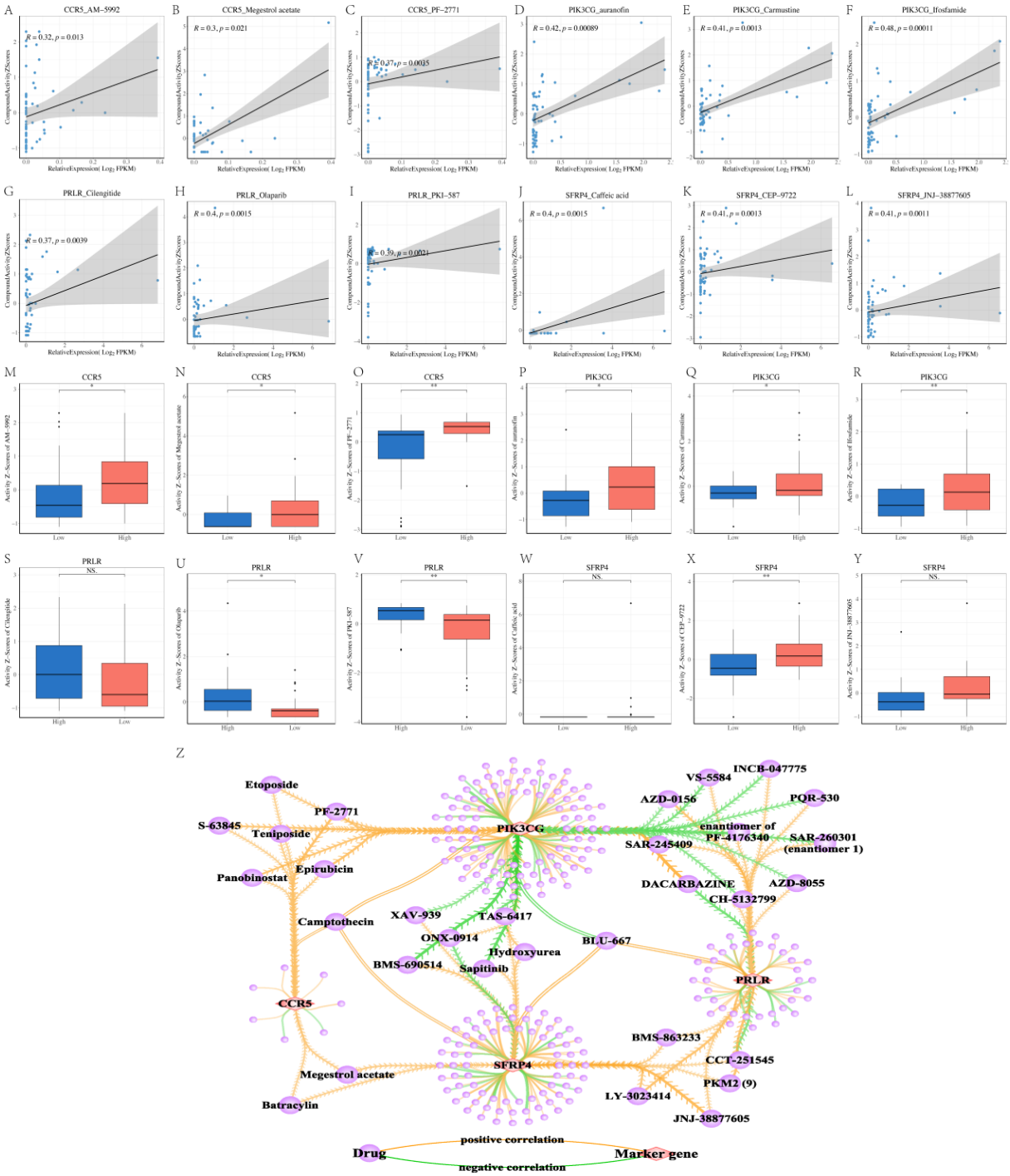

Figure 4. (A-L) Drugs highly correlated with marker genes

(M-Y) Drug-sensitizing activity of significant drugs in different risk groups of marker gene. (Z) Relationship network of marker gene and drug. Where the thicker line represents the higher correlation.

3.5 Immune Infiltration Analysis

The PI dataset was analyzed according to CIBERSORT, selecting samples with p-value < 0.05 as significantly relevant, resulting in a total of 12 case samples and 10 control samples. The scores of immune cells in the samples are shown in Fig 5A, and the differences among 22 immune cells across different sample types were analyzed using the Wilcoxon test (Fig 5B). As a result, plasma cells, NK cells resting, and mast cells activated were highly enriched and significantly different in the disease group of PI. T cells follicular helper, NK cells activated, and mast cells resting were highly enriched and significantly different in the normal group. A matrix of 6 significantly different immune cell abundance scores was extracted, and these immune cells and their correlations with other immune cells were analyzed using Pearson correlation coefficients (Fig 5A). Additionally, the relationship between these immune cells and the 4 marker genes was predicted (Fig 5B).

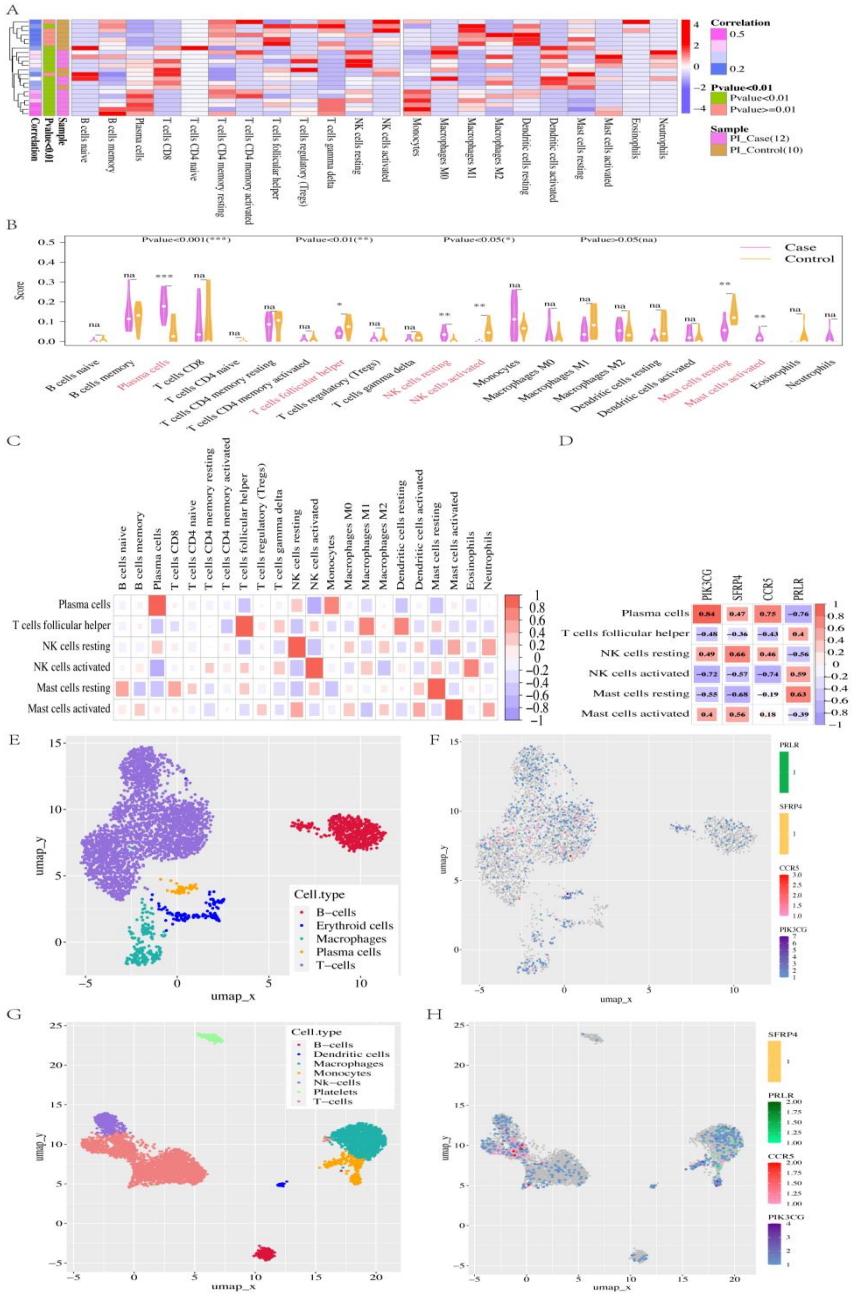

Figure 5. Immune cell infiltration analysis

(A) Heatmap of immune cell enrichment in case and control samples; (B) Differential enrichment of immune cells in case and control groups. Horizontal coordinates are immune cells and vertical coordinates are enrichment scores for infiltration analysis. (C) Significant differential immune cell correlation analysis; (D) The marker gene vs differential immune cell analysis; (E) clustering of single cells in bone; (F) expression of marker genes in single cells in bone; (G) clustering of single cells in PBMC; (H) expression of marker genes in single cells of PBMC.

The results showed that T cells follicular helper was significantly positively correlated with macrophages M1 and dendritic cells resting (cor > 0.6). Plasma cells were significantly negatively correlated with NK cells activated (cor = -0.6027) and significantly positively correlated with monocytes (cor = 0.6485). NK cells activated were significantly negatively correlated with plasma cells (cor = -0.6027) and positively correlated with eosinophils (cor = 0.6712) (Fig 5C). CCR5 and PIK3CG were significantly positively correlated with plasma cells (cor > 0.5), with correlation coefficients of 0.7536 and 0.8386, respectively, and negatively correlated with NK cells activated (cor = -0.7407 and -0.7188, respectively). PRLR was significantly positively correlated with mast cells resting (cor = 0.6294) and significantly negatively correlated with plasma cells activated (cor = -0.7407 and -0.7188) (Fig 5D). SFRP4 was significantly positively correlated with NK cells resting (cor = 0.6558) and negatively correlated with mast cells resting (cor = -0.6823) (Fig 5D).

3.6 Expression Analysis of Marker Gene in Single Cells of Bone and PBMCs

To analyze the clustering of peri-implantitis and osteoporosis single cells, the single-cell analysis results of bone marrow and PBMC were extracted from the HPA database. The expression of the four marker genes in bone and PBMC was obtained. From the results, the main cell groups in the bone were B-cells, erythroid cells, macrophages, plasma cells, and T-cells (Fig 5E). PIK3CG was highly expressed in plasma cells and T-cells; CCR5 was mainly highly expressed in T-cells and macrophages; PRLR and SFRP4 were lowly expressed in the cell clusters of the bone (Fig 5F). For PBMC, the following cell populations were mainly enriched: B-cells, dendritic cells, macrophages, monocytes, NK-cells, plasma cells, platelets, and T-cells (Fig 5G). In PBMC, PIK3CG was highly expressed in NK-cells, macrophages, T-cells, and monocytes; CCR5 was expressed mainly in T-cells; PRLR was highly expressed in macrophages; and SFRP4 was lowly expressed in the cell clusters of PBMC (Fig 5H).

Based on the analysis of immune infiltration, it was hypothesized that in the bone of patients with PI disease, PIK3CG mainly plays a regulatory role on plasma cells and is positively correlated, while in the blood, it mainly acts on NK-cells and is negatively correlated. From the previous marker gene-related pathway results, it was obtained that PIK3CG and PRLR are involved in regulating the PI3K-Akt signaling pathway, SFRP4 is involved in regulating the Wnt signaling pathway, and PRLR and CCR5 are involved in regulating the cytokine-cytokine receptor signaling pathway. The pathway maps of these three pathways were downloaded from the KEGG database, and cross-talk genes were mapped to the pathways to obtain the roles of marker genes in the pathways (Fig 6A-C).

3.7 The Three Mediated Signaling Pathways

PRLR and PIK3CG regulate the PI3K-Akt signaling pathway by activating other genes and compounds (Fig 6A). In the PI3K-Akt signaling pathway, PRLR affects C05981 (Phosphatidylinositol-3,4,5-trisphosphate) through the action of PIK3CA, and PIK3CG directly affects C05981, which promotes the expression of AKT1 and PDPK1, thereby affecting disease development. SFRP4 regulates the Wnt signaling pathway by mainly inhibiting the expression of related genes (Fig 6B). The CCR5-translated protein is an important co-receptor for the entry of macrophage viruses into host cells, and the gene is located in the chemokine receptor gene cluster region, which in turn affects the cytokine-cytokine receptor interaction pathway by being regulated by other family genes (Fig 6C).

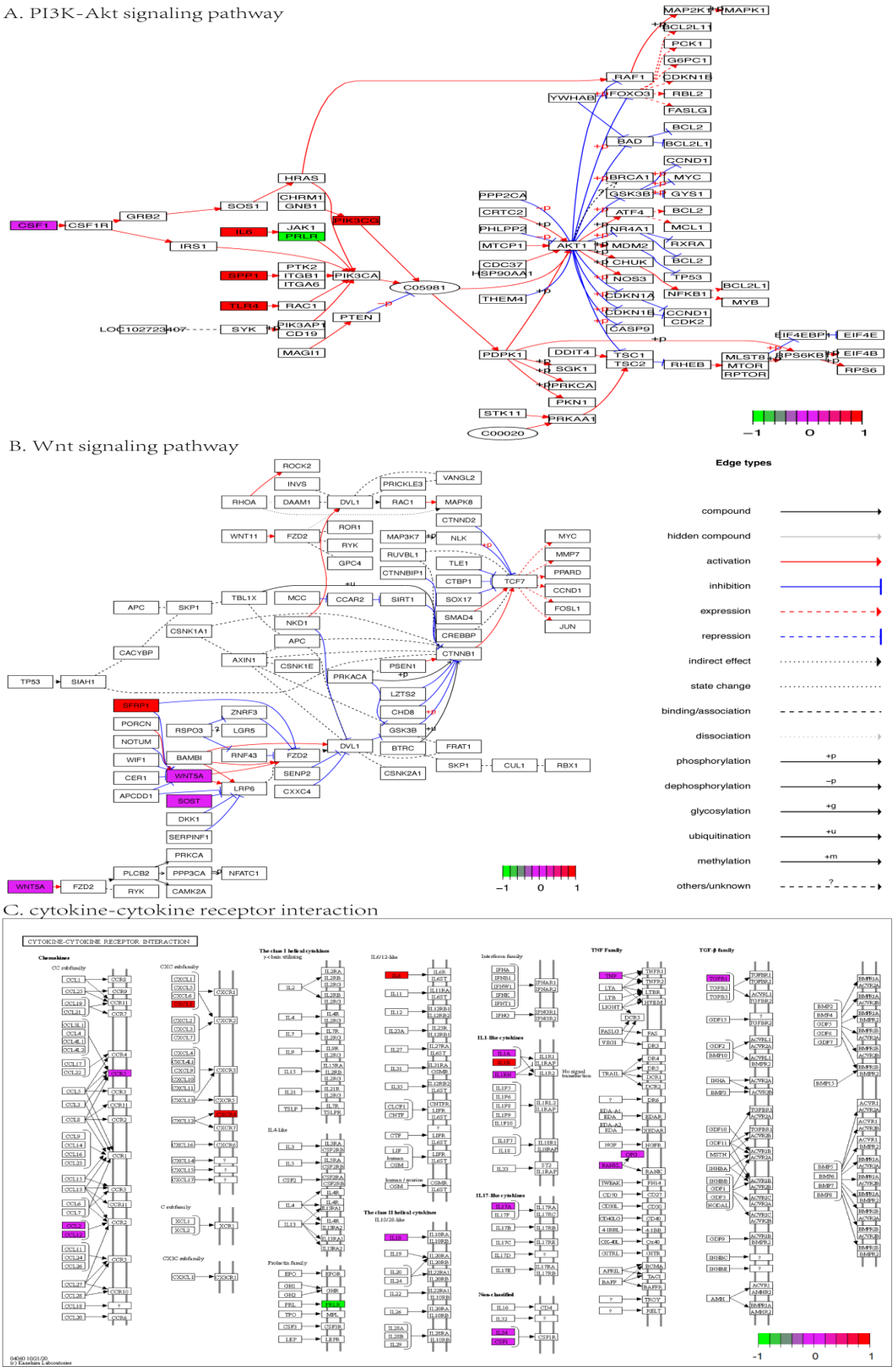

Figure 6. Regulation of PRLR, PIK3CG and SFRP4 in pathway

(A) PI3K-Akt signaling pathway; (B) Wnt signaling pathway. red nodes in the figure are up-regulated genes, green nodes are down-regulated genes, and pink nodes are genes that exist only in the DisGeNET database. (C) Regulation of CCR5 in Cytokine-cytokine receptor interaction.

4. Discussion

Recent research has highlighted the crucial roles of four marker genes—PIK3CG, SFRP4, CCR5, and PRLR—in the interconnected pathologies of PI and OP. The gene CCR5 is a chemokine receptor that binds to certain inflammatory molecules and mediates cell migration and activation (28). CCR5 mRNA and protein levels are higher in PI sites than in healthy sites (28). CCR5 may be involved in the recruitment and activation of inflammatory cells, such as macrophages and T cells, to the peri-implant tissues, contributing to tissue damage and bone resorption (28). CCR5 was also found to be expressed on both osteoblasts and osteoclasts, as well as on immune cells that affect bone remodeling. CCR5 mediates the effects of CCL3, CCL4, and CCL5 on osteoblast and osteoclast function, such as chemotaxis, survival, differentiation, and resorption. CCR5 and its ligands are elevated in osteoporosis patients, and play a role in osteoporosis by affecting bone metabolism and inflammation (29). CCR5 antagonists may have therapeutic potential for osteoporosis by inhibiting bone resorption and inflammation (29). Phosphoinositide 3-kinase gamma (PI3KCG) activates signaling molecules of inflammation, as it is a lipid kinase in leukocytes, which can generate phosphatidylinositol 3,4,5-trisphosphate, whereby it has pivotal roles in myeloid and lymphocyte cell migration (30). Until now, there is no clinical data linking PI3KCG with PI; however, another bioinformatics study revealed this Gene to be a hub gene in the interrelationship between PI and diabetes (31). Similarly, only a bioinformatics approach showed PI3KCG to be related with OP (32). Nevertheless, the potential role of this gene in PI and OP might underline the autoimmunity of both conditions, as PI3KCG is highly associated with autoimmune disease and inflammation (30). Thus, the findings of PIKCG as an important marker gene appears plausible and an interesting future approach. Secreted Frizzled Receptor Protein 4 (SFRP4) is a receptor for Wnt ligands, whereby it is relevant in bone metabolism, especially as mediator of periosteal stem cell/progenitor expansion and differentiation (33). No previous report on its potential role in PI is available. For OP, several studies have been reported in this context. For example, a review article described that SFRP4, as an effector of cortical and trabecular bone metabolism, would be related to osteoporosis of the cortical bone (34). Moreover, it has been shown that SFRP4-dependent Wnt signaling would have a direct effect on age-related bone loss and bone formation (35). A Korean study showed that a polymorphism of SRFP4 would be associated with bone mineral density in postmenopausal women (36). Taken together, although no literature is available for PI, the role of SRFP4 in bone metabolism and bone loss could explain its relevance in the interplay between PI and OP. PRLR is the prolactin receptor, which is associated with a modulation of a variety of inflammatory and immune processes, and thereby with different types of cancer (37)(38). One study, which investigated gingival tissue samples of PI patients found PRLR to be one out of six genes in the regulated ceRNA network (39). A recent review illustrated the multifarious occurrence of PRLR and its potential relevance in distinct cell types, including bone. Thus, a potential relevance in context of OP is also conceivable. Taken together, all of the four potential marker genes indicate a relationship between OP and PI via bone metabolism, inflammation and autoimmunity. Thereby, both diseases appear to have a distinct similarity.

The interplay between PI and OP is significantly influenced by the regulation of three crucial signaling pathways: PI3K-Akt signaling, Wnt signaling, and cytokine-cytokine receptor interaction, each playing a distinctive yet interconnected role in both conditions. The PI3K-Akt signaling pathway plays a crucial role in the pathogenesis of PI, particularly in regulating inflammatory responses and bone resorption (40). It mediates the effects of proinflammatory cytokines, such as Tumor Necrosis Factor-alpha (TNF-α), Interleukin-6 (IL-6), and Interleukin-8 (IL-8), which influence the expression of adhesion molecules, chemokines, and matrix metalloproteinases (MMPs) (41). These factors are involved in the recruitment and activation of inflammatory cells and the degradation of the extracellular matrix (41). Additionally, the PI3K/AKT pathway enhances osteoclastogenesis by stimulating the expression of Nuclear Factor of Activated T-cells cytoplasmic 1 (NFATc1), a key transcription factor for osteoclast differentiation, and inhibits osteoclast apoptosis by activating anti-apoptotic proteins such as Bcl-2 and Bcl-xL (42). PI3K/AKT signaling pathway is involved in the inhibition of OP through promoting osteoblast function and bone formation (43,44). In osteoporosis, the activation of PI3K/AKT signaling is impaired, leading to reduced osteoblast proliferation, differentiation, and mineralization (45). In cultured osteoblasts, the inhibition of PI3K/AKT signaling by a specific inhibitor reduces cell proliferation, differentiation, and mineralization, and increases apoptosis (45).

While this research on PI and OP provides novel insights, there are certain limitations that need to be acknowledged. Firstly relying on computational analyses may oversimplify the intricate interplay between genetic molecular and environmental factors that impact bone health. These analyses are bound by predetermined assumptions, and may

not fully capture the complexity of biological systems in vivo. Another important limitation is the lack of diverse genetic and demographic data, which could limit the generalizability of the findings across different populations. Additionally an exclusive focus on genes and pathways might overlook other significant factors contributing to these diseases. The translation of model based discoveries into practice poses its own challenges necessitating extensive validation through clinical trials to establish the effectiveness and safety of potential treatments. Moreover, considering the nature of bone remodeling influenced by age hormonal changes and comorbidities adds further complexity and may restrict the applicability of study findings. Lastly developing treatment strategies for PI and OP is challenging due, to their multifactorial nature Influenced by lifestyle choices medications used and overall systemic health considerations.

The research conducted on PI and OP has potential implications for clinical practice and future investigations. The discovery of genes such as PIK3CG, SFRP4, CCR5 and PRLR as well as the understanding of crucial pathways like PI3K Akt, Wnt signaling and cytokine cytokine receptor interactions offers a solid foundation in molecular studies that could potentially revolutionize current diagnostic methods and treatment approaches. These findings provide opportunities for the development of targeted therapies that may prove effective with fewer side effects than traditional treatments. For example exploring modulators of the Wnt pathway or PI3K Akt signaling could lead to medications designed specifically to address bone remodeling imbalances observed in both PI and OP. Moreover establishing connections between these two conditions allows for a more integrated approach towards managing bone related diseases. By understanding shared factors, comprehensive treatment plans can be developed to address both conditions simultaneously especially in patients who have a predisposition to both ailments. Additionally the genetic markers identified in this study could serve as tools for early detection and risk assessment purposes empowering healthcare providers with proactive strategies, for preventive care.

5. Conclusion

The current study showed that the marker genes PIK3CG, SFRP4, CCR5, and PRLR, along with the PI3K-Akt, Wnt, and cytokine-cytokine receptor interaction pathways, play pivotal roles in the pathogenesis of PI and OP. These findings not only enhance the understanding of the genetic and molecular underpinnings of these conditions, but also open avenues for targeted therapeutic interventions. The exploration of these genes and pathways offers valuable insights into potential strategies for treatment and prevention. However, further research is essential to translate these findings into clinical practice and to ensure their effectiveness and applicability in diverse patient populations.

Acknowledgements

Nothing to declare.

References

[1] Giro, G., Chambrone, L., Goldstein, A., Rodrigues, J. A., Zenóbio, E., Feres, M., et al. (2015). Impact of osteoporosis in dental implants: a systematic review. *World Journal of Orthopaedics, 6*(2), 311. https://doi.org/10.5312/wjo.v6.i2.311

[2] De Medeiros, F., Kudo, G. A. H., Leme, B. G., Saraiva, P. P., Verri, F. R., Honório, H. M., et al. (2018). Dental implants in patients with osteoporosis: a systematic review with meta-analysis. *International Journal of Oral and Maxillofacial Surgery, 47*(4), 480–491. https://doi.org/10.1016/j.ijom.2017.05.021

[3] Guobis, Z., Pacauskiene, I., & Astramskaite, I. (2016). General diseases influence on peri-implantitis development: a systematic review. *Journal of Oral and Maxillofacial Research*, 7(3). https://doi.org/10.5037/jomr.2016.7305

[4] Dvorak, G., Arnhart, C., Heuberer, S., Huber, C. D., Watzek, G., & Gruber, R. (2011). Peri-implantitis and late implant failures in postmenopausal women: a cross-sectional study: Peri-implantitis in postmenopausal women. *Journal of Clinical Periodontology, 38*(10), 950–955. https://doi.org/10.1111/j.1600-051X.2011.01772.x

[5] Dreyer, H., Grischke, J., Tiede, C., Eberhard, J., Schweitzer, A., Toikkanen, S. E., et al. (2018). Epidemiology and risk factors of peri-implantitis: A systematic review. *Journal of Periodontal Research*, *53*(5), 657–681. https://doi.org/10.1111/jre.12562

[6] Corcuera-Flores, J. R., Alonso-Domínguez, A. M., Serrera-Figallo, M. Á., Torres-Lagares, D., Castellanos-Cosano, L., & Machuca-Portillo, G. (2016). Relationship between osteoporosis and marginal bone loss in osseointegrated implants: A 2-year retrospective study. *Journal of Periodontology, 87*(1), 14–20. https://doi.org/10.1902/jop.2015.150229

[7] Smeets, R., Henningsen, A., Jung, O., Heiland, M., Hammächer, C., & Stein, J. M. (2014). Definition, etiology, prevention and treatment of peri-implantitis – a review. *Head & Face Medicine, 10*(1), 34. https://doi.org/10.1186/1746-160X-10-34

[8] Schwarz, F., Derks, J., Monje, A., & Wang, H. (2018). Peri-implantitis. *Journal of Clinical Periodontology*, 45(S20). https://doi.org/10.1111/jcpe.12954

[9] Clowes, J. A., Riggs, B. L., & Khosla, S. (2005). The role of the immune system in the pathophysiology of osteoporosis. *Immunological Reviews, 208*(1), 207–227. https://doi.org/10.1111/j.0105-2896.2005.00334.x

[10] Kensara, A., Hefni, E., Williams, M. A., Saito, H., Mongodin, E., & Masri, R. (2021). Microbiological profile and human immune response associated with peri-implantitis: A systematic review. *Journal of Prosthodontics, 30*(3), 210–234. https://doi.org/10.1111/jopr.13270

[11] Pietschmann, P., Mechtcheriakova, D., Meshcheryakova, A., Föger-Samwald, U., & Ellinger, I. (2016). Immunology of osteoporosis: a mini-review. *Gerontology, 62*(2), 128–137. https://doi.org/10.1159/000431091

[12] Petković, A. B., Matić, S. M., Stamatović, N. V., Vojvodić, D. V., Todorović, T. M., Lazić, Z. R., et al. (2010). Proinflammatory cytokines (IL-1β and TNF-α) and chemokines (IL-8 and MIP-1α) as markers of peri-implant tissue condition. *International Journal of Oral and Maxillofacial Surgery, 39*(5), 478–485. https://doi.org/10.1016/j.ijom.2010.01.014

[13] Zheng, S. X., Vrindts, Y., Lopez, M., De Groote, D., Zangerlé, P. F., Collette, J., et al. (1997). Increase in cytokine production (IL-1β, IL-6, TNF-α but not IFN-γ, GM-CSF or LIF) by stimulated whole blood cells in postmenopausal osteoporosis. *Maturitas, 26*(1), 63–71. https://doi.org/10.1016/S0378-5122(96)01080-8

[14] Contaldo, M., Itro, A., Lajolo, C., Gioco, G., Inchingolo, F., & Serpico, R. (2020). Overview on osteoporosis, periodontitis and oral dysbiosis: the emerging role of oral microbiota. *Applied Sciences, 10*(17), 6000. https://doi.org/10.3390/app10176000

[15] Hernández-Vigueras, S., Martínez-Garriga, B., Sánchez, M. C., Sanz, M., Estrugo-Devesa, A., Vinuesa, T., et al. (2016). Oral microbiota, periodontal status, and osteoporosis in postmenopausal females. *Journal of Periodontology, 87*(2), 124–133. https://doi.org/10.1902/jop.2015.150365

[16] Sgolastra, F., Petrucci, A., Severino, M., Gatto, R., & Monaco, A. (2015). Smoking and the risk of peri-implantitis: A systematic review and meta-analysis. *Clinical Oral Implants Research, 26*(4). https://doi.org/10.1111/clr.12319

[17] Ratajczak, A. E., Szymczak-Tomczak, A., Rychter, A. M., Zawada, A., Dobrowolska, A., & Krela-Kaźmierczak, I. (2021). Impact of cigarette smoking on the risk of osteoporosis in inflammatory bowel diseases. *Journal of Clinical Medicine, 10*(7), 1515. https://doi.org/10.3390/jcm10071515

[18] Li, S., Zhou, C., Pelekos, G., Ziebolz, D., Schmalz, G., & Qin, Z. (2021). Similarity and potential relation between periimplantitis and rheumatoid arthritis on transcriptomic level: Results of a bioinformatics study. *Frontiers in Immunology, 12*, 702661. https://doi.org/10.3389/fimmu.2021.702661

[19] Lei, H., Chen, X., Wang, Z., Xing, Z., Du, W., Bai, R., et al. (2023). Exploration of the underlying comorbidity mechanism in psoriasis and periodontitis: A bioinformatics analysis. *Hereditas, 160*(1), 7. https://doi.org/10.1186/s41065-023-00266-z

[20] He, Z., Jiang, Q., Li, F., & Chen, M. (2021). Crosstalk between venous thromboembolism and periodontal diseases: A bioinformatics analysis. *Disease Markers*, 2021. https://doi.org/10.1155/2021/1776567

[21] Wang, X., Shi, N., Wu, B., Yuan, L., Chen, J., Ye, C., et al. (2022). Bioinformatics analysis of gene expression profile and functional analysis in periodontitis and Parkinson's disease. *Frontiers in Aging Neuroscience*, 14, 1029637. https://doi.org/10.3389/fnagi.2022.1029637

[22] Kang, J., Kwon, E. J., Yu, Y., Kim, Y., & Kim, Y. H. (2022). Identification of shared genes and pathways in periodontitis and type 2 diabetes by bioinformatics analysis. *Frontiers in Endocrinology*, 12, 724278. https://doi.org/10.3389/fendo.2021.724278

[23] Liu, S., Wang, Z., Zhu, R., Wang, F., Cheng, Y., & Liu, Y. (2021). Three differential expression analysis methods for RNA sequencing: limma, EdgeR, DESeq2. *Journal of Visualized Experiments*, (175), e62528. https://doi.org/10.3791/62528

[24] Kolde, R., & Kolde, M. R. (2015). Package 'pheatmap'. *R Package*, 1(7), 790.

[25] Harrell Jr, F. E., Harrell Jr, M. F. E., & Hmisc, D. (2017). Package 'rms'. *Vanderbilt University*, 229, Q8.

[26] Bi, G., Li, R., Liang, J., Hu, Z., & Zhan, C. (2020). A nomogram with enhanced function facilitated by nomogramEx and nomogramFormula. *Annals of Translational Medicine*, 8(4). https://doi.org/10.21037/atm.2020.01.71

[27] Luo, W., & Brouwer, C. (2013). Pathview: An R/Bioconductor package for pathway-based data integration and visualization. *Bioinformatics, 29*(14), 1830–1831. https://doi.org/10.1093/bioinformatics/btt285

[28] Venza, I., Visalli, M., Cucinotta, M., De Grazia, G., Teti, D., & Venza, M. (2010). Proinflammatory gene expression at chronic periodontitis and peri-implantitis sites in patients with or without type 2 diabetes. *Journal of Periodontology, 81*(1), 99–108. https://doi.org/10.1902/jop.2009.090358

[29] Farangis, F., Majid, M., Gholamhossein, H., Soudeh, K., Hossein, K., Zahra, A., et al. (2017). CC chemokines CCL2, CCL3, CCL4 and CCL5 are elevated in osteoporosis patients. *Journal of Biomedical Research, 31*(5), 468. https://doi.org/10.7555/JBR.31.20150166

[30] Venable, J. D., Ameriks, M. K., Blevitt, J. M., Thurmond, R. L., & Fung-Leung, W. P. (2010). Phosphoinositide 3-kinase gamma (PI3Kγ) inhibitors for the treatment of inflammation and autoimmune disease. *Recent Patents on Inflammation & Allergy Drug Discovery, 4*(1), 1–15. https://doi.org/10.2174/187221310789895603

[31] Yu, T., Acharya, A., Mattheos, N., Li, S., Ziebolz, D., Schmalz, G., et al. (2019). Molecular mechanisms linking peri-implantitis and type 2 diabetes mellitus revealed by transcriptomic analysis. *PeerJ*, *7*, e7124. https://doi.org/10.7717/peerj.7124

[32] Chai, Y., Tan, F., Ye, S., Liu, F., & Fan, Q. (2019). Identification of core genes and prediction of miRNAs associated with osteoporosis using a bioinformatics approach. *Oncol Lett*, *17*(1), 468–481. https://doi.org/10.3892/ol.2018.9508

[33] Chen, R., Baron, R., & Gori, F. (2022). Sfrp4 and the biology of cortical bone. *Curr Osteoporos Rep*, *20*(2), 153–161. https://doi.org/10.1007/s11914-022-00727-w

[34] Brommage, R., & Ohlsson, C. (2018). Translational studies provide insights for the etiology and treatment of cortical bone osteoporosis. *Best Pract Res Clin Endocrinol Metab*, *32*(3), 329–340. https://doi.org/10.1016/j.beem.2018.02.006

[35] Haraguchi, R., Kitazawa, R., Mori, K., Tachibana, R., Kiyonari, H., Imai, Y., et al. (2016). sFRP4-dependent Wnt signal modulation is critical for bone remodeling during postnatal development and age-related bone loss. *Sci Rep*, *6*(1), 25198. https://doi.org/10.1038/srep25198

[36] Lee, D. Y., Kim, H., Ku, S. Y., Kim, S. H., Choi, Y. M., & Kim, J. G. (2010). Association between polymorphisms in Wnt signaling pathway genes and bone mineral density in postmenopausal Korean women. *Menopause*, *17*(5), 1064–1070. https://doi.org/10.1097/gme.0b013e3181da4da3

[37] Liang, J., Deng, Y., Zhang, Y., Wu, B., & Zhou, J. (2022). PRLR and CACNA2D1 impact the prognosis of breast cancer by regulating tumor immunity. *J Pers Med*, *12*(12), 2086. https://doi.org/10.3390/jpm12122086

[38] Suarez, A. L. P., López-Rincón, G., Martínez Neri, P. A., & Estrada-Chávez, C. (2015). Prolactin in inflammatory response. In M. Diakonova (Ed.), *Recent advances in prolactin research* (Vol. 846, pp. 243–264). Cham: Springer International Publishing. https://doi.org/10.1007/978-3-319-12114-7_11

[39] Zhou, H., Chen, D., Xie, G., Li, J., Tang, J., & Tang, L. (2020). lncRNA-mediated ceRNA network was identified as a crucial determinant of differential effects in periodontitis and periimplantitis by high-throughput sequencing. *Clin Implant Dent Relat Res*, *22*(3), 424–450. https://doi.org/10.1111/cid.12911

[40] Oh, J., Kim, Y., Son, H., Kim, Y. H., & Kim, H. (2023). Comparative transcriptome analysis of periodontitis and peri-implantitis in human subjects. *J Periodontol*, *Oct 3*, JPER.23-0289.

[41] Glaviano, A., Foo, A. S. C., Lam, H. Y., Yap, K. C. H., Jacot, W., Jones, R. H., et al. (2023). PI3K/AKT/mTOR signaling transduction pathway and targeted therapies in cancer. *Mol Cancer*, *22*(1), 138. https://doi.org/10.1186/s12943-023-01827-6

[42] Moon, J. B., Kim, J. H., Kim, K., Youn, B. U., Ko, A., Lee, S. Y., et al. (2012). Akt induces osteoclast differentiation through regulating the GSK3β/NFATc1 signaling cascade. *J Immunol*, *188*(1), 163–169. https://doi.org/10.4049/jimmunol.1101254

[43] Zhou, R. P., Lin, S. J., Wan, W. B., Zuo, H. L., Yao, F. F., Ruan, H. B., et al. (2016). Chlorogenic acid prevents

osteoporosis by Shp2/PI3K/Akt pathway in ovariectomized rats. *PLoS One*, *11*(12), e0166751. https://doi.org/10.1371/journal.pone.0166751

[44] Wang, H., Zhao, W., Tian, Q. J., Xin, L., Cui, M., & Li, Y. K. (2020). Effect of lncRNA AK023948 on rats with postmenopausal osteoporosis via PI3K/AKT signaling pathway. *Eur Rev Med Pharmacol Sci*, *24*(5), 2181–2188.

[45] Xi, J. C., Zang, H. Y., Guo, L. X., Xue, H. B., Liu, X. D., Bai, Y. B., et al. (2015). The PI3K/AKT cell signaling pathway is involved in regulation of osteoporosis. *J Recept Signal Transduct*, *35*(6), 640–645. https://doi.org/10.3109/10799893.2015.1041647

Copyrights

Copyright for this article is retained by the author(s), with first publication rights granted to the journal.

This is an open-access article distributed under the terms and conditions of the Creative Commons Attribution license (http://creativecommons.org/licenses/by/4.0/).